Olefin Polymerization Hot Paper

How to cite: *Angew. Chem. Int. Ed.* **2020**, *59*, 14296–14302
International Edition: doi.org/10.1002/anie.202004763
German Edition: doi.org/10.1002/ange.202004763

Ultrahigh Branching of Main-Chain-Functionalized Polyethylenes by Inverted Insertion Selectivity

Yuxing Zhang, Chaoqun Wang, Stefan Mecking, and Zhongbao Jian**

Abstract: *Branched polyolefin microstructures resulting from so-called "chain walking" are a fascinating feature of late transition metal catalysts; however, to date it has not been demonstrated how desirable branched polyolefin microstructures can be generated thereby. We demonstrate how highly branched polyethylenes with methyl branches (220 Me/1000 C) exclusively and very high molecular weights (ca. 10^6 g mol^{-1}), reaching the branch density and microstructure of commercial ethylene–propylene elastomers, can be generated from ethylene alone. At the same time, polar groups on the main chain can be generated by in-chain incorporation of methyl acrylate. Key to this strategy is a novel rigid environment in an α-diimine Pd^{II} catalyst with a steric constraint that allows for excessive chain walking and branching, but restricts branch formation to methyl branches, hinders chain transfer to afford a living polymerization, and inverts the regioselectivity of acrylate insertion to a 1,2-mode.*

Polyolefins, such as polyethylene (PE) and polypropylene (PP), are the largest scale synthetic polymers and are ubiquitous in modern society.[1–4] Since Ziegler and Natta's discoveries on metal-catalyzed olefin polymerization, a variety of advanced polyethylene materials have been developed. Linear polyethylene with no or very few branches (for example, high-density polyethylene (HDPE)), as well as substantially branched linear low-density polyethylenes (LLDPEs), and ethylene–propylene (EP) elastomers, are produced industrially (Figure 1). The branches in the latter originate from 1-olefin comonomer (C_4, C_6, or C_8 in LLDPEs, and C_3 in EP elastomers). Compared to the traditional catalysts used in these reactions, late transition metal catalysts possess two distinct features: they are capable of copolymerization with polar monomers, and they are capable of generating branched microstructures from ethylene monomer alone by a unique chain walking mechanism that generates methyl branches predominantly, but also higher branches.[5–22]

The generation of branches from ethylene as the sole building block is attractive as it can simplify processes and eliminate the need for more costly comonomers. Furthermore, ethylene can be generated by dehydration of carbohydrate-based bioethanol, while 1-olefins require additional steps. However, to date branch densities and branch patterns fall short of the microstructures desired. Extensive investigations with respect to different late transition metal catalysts, such as palladium catalysts, primarily yielded branch densities of 130/1000 C atoms at the most.[23] By contrast, typical EP elastomers contain 200 or more methyl groups/1000 carbon atoms.

Herein, we reveal that tailoring of the steric environment of the active site enables the generation of highly branched structures. The underlying mechanism offers unique selectivity for the formation of small methyl branches only, and incorporation of polar monomers exclusively in the main chain (Figure 1), and in a living polymerization.

Catalyst Design. As a rationale for catalyst design, we aimed for a defined steric environment of the active site. To provide such a defined environment, we pursued a highly rigid ligand structure by matching the diimine backbone and the *N*-aryl groups, which places the active site in a symmetrical wedge. This was achieved by means of a novel α-diimine

[*] Y. Zhang, C. Wang, Prof. Dr. Z. Jian
State Key Laboratory of Polymer Physics and Chemistry, Changchun Institute of Applied Chemistry, Chinese Academy of Sciences
Renmin Street 5625, Changchun 130022 (China)
and
University of Science and Technology of China
Hefei 230026 (China)
E-mail: zbjian@ciac.ac.cn
Prof. Dr. S. Mecking
Chair of Chemical Materials Science, Department of Chemistry
University of Konstanz
78457 Konstanz (Germany)
E-mail: stefan.mecking@uni-konstanz.de
Supporting information and the ORCID identification number(s) for the author(s) of this article can be found under: https://doi.org/10.1002/anie.202004763.

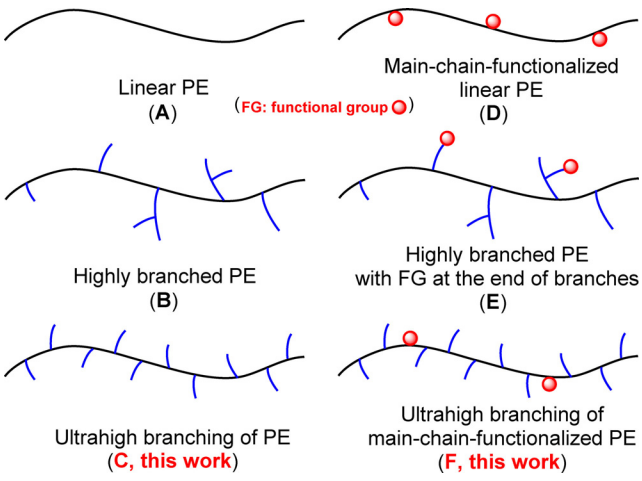

Figure 1. (Functionalized) polyethylene architectures from ethylene polymerization and copolymerization with polar comonomers.

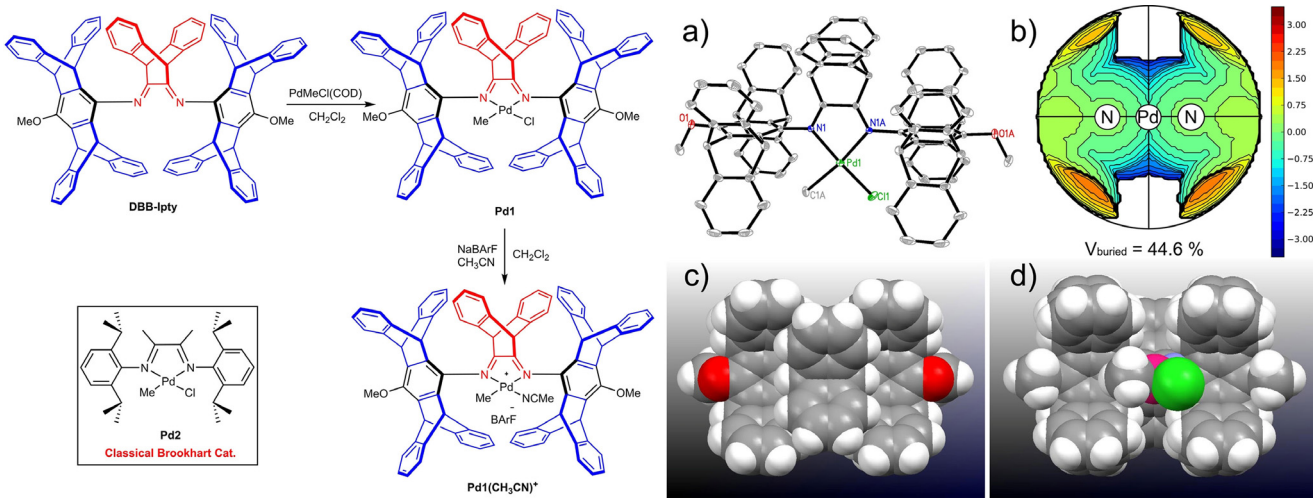

Figure 2. Left: Synthesis of α-diimine Pd^{II} complex **Pd1** with Ipty axial substituents and DBB backbone. Right: a) molecular structure of **Pd1** drawn with 30% probability ellipsoids; b) steric map of **Pd1** (view from bottom to top); c) space-filling model of **Pd1** (view from top to bottom, that is from the back side of the molecule); d) space-filling model of **Pd1** (view from bottom to top, that is from the front of the molecule).

ligand **DBB-Ipty** with a bulky dibenzobarrelene (DBB) backbone and bulky axial pentiptycenyl (Ipty) substituents (for detailed synthetic procedures and characterization data, see the Supporting Information). Reaction of **DBB-Ipty** with [PdMeCl(COD)] afforded the desired Pd^{II} complex **Pd1** in an excellent yield of 88% (Figure 2, left). As a benchmark, Brookhart's Pd^{II} complex **Pd2** was also prepared, according to reported procedures.[17]

The structure and purity of **Pd1** was fully determined by nuclear magnetic resonance (NMR) spectroscopy, elemental analysis, and X-ray diffraction analysis. The key Pd-Me ^{1}H resonance arises at 0.05 ppm. This is at notably higher field relative to other related α-diimine Pd^{II} complexes,[24,25] indicating shielding by the distal iptycene aryl rings (see the proceeding text). Single-crystal X-ray diffraction structure analysis reveals that the square-planar **Pd1** is highly symmetrical, rigid, and sterically encumbered, as reflected by a buried volume V_{Bur} of 45% (Figure 2, right: a and b).[26] Notably, this V_{Bur}% is less than the value (49%) of **DBB-iPr-Pd** reported by Gao (Supporting Information),[24] but the DBB backbone also efficiently inhibits the rotation of axial Ipty substituents (Figure 2, right: c). As a result, the crucial Pd-Me group is buried by the axial Ipty substituents because it is placed at the center of two wedges (Figure 2, right: d). This special rigid framework protects the axial sites of active centers and, thus, is prone to retard the associative displacement chain transfer.

Ultrahigh Branching of Polyethylenes. The ethylene polymerization catalytic properties of **Pd1** activated with sodium tetrakis[3,5-bis(trifluoromethyl)phenyl]borate (NaBArF) were studied at variable conditions (Table 1). Remarkably, **Pd1** is active over a very broad range of polymerization temperatures from 0 °C up to 130 °C, demonstrating an outstanding thermal stability of the catalyst. With increasing temperature, the catalytic activity increases and reaches a maximum value at 70 °C corresponding to a very high turnover frequency of 8×10^4 mol(ethylene) mol(Pd)$^{-1}$ h^{-1} (Table 1, entry 5). Productivities are lower at even higher temperatures, indicating that partial catalyst deactivation occurs in the course of these 0.5 hour experiments. Studies of polymerizations with variable time spans, from 30 minutes up to 8 hours at 50 °C, further demonstrated that catalyst activity is retained over several hours and extremely high molecular weights can be achieved ($M_n = 904$ kg mol^{-1}, $M_w = 1573$ kg mol^{-1}; Table 1, entries 4, 9, and 10). For comparison, under otherwise identical conditions **Pd2** is considerably less active and affords much lower polymer molecular weight. At a high polymerization temperature of 90 °C, **Pd2** is immediately deactivated completely and affords traces of polymer, in strong contrast to our catalyst **Pd1** (Table 1, entries 6 vs. 14). At low temperatures, the polymerization is living (see proceeding text) and polymer molecular weights are limited by the rate of chain growth. Consequently, polymer molecular weights increase with increasing temperature. Only at 50 °C and at higher temperatures do chain-transfer events occur, as evidenced by a broadening of the molecular weight distribution. Nonetheless, even at 50 °C very few chain-transfer events occur at an active site (less than one per hour), as reflected by an increase of average polymer molecular weights even after several hours of polymerization (Table 1, entries 4, 9, and 10).

Remarkably, **Pd1** affords unprecedented extremely high degrees of branching of 220/1000 C, as revealed by ^{1}H and ^{13}C NMR analysis (Table 1, entry 1; for full polymer characterization data, see the Supporting Information). This value greatly exceeds the branching behavior reported for α-diimine Pd^{II} catalysts to date (< 130/1000 C). As a further unique feature, branching decreases with increasing polymerization temperature, and does so to a dramatic extent. While an ultrahigh degree of branching of 220/1000 C is observed at 0 °C, at 130 °C only 125/1000 C is observed. This contrasts the general picture observed for α-diimine Pd^{II} catalysts to date, which display degrees of branching independent of reaction conditions;[27] namely, the total number of branches is invariant with temperature.[24,28,29] Indeed, the reference experiments with Brookhart's classical α-diimine Pd^{II} catalyst

Table 1: Effect of temperature on ethylene polymerization with α-diimine **Pd1** and **Pd2**.[a]

Entry	Cat.	T [°C]	Yield [g]	Act. [$\times 10^6$][b]	M_n [$\times 10^4$][c]	M_w [$\times 10^4$][c]	M_w/M_n[c]	Brs[d]	Me content [%][e]	T_g[f] [°C]
1[g]	**Pd1**	0	0.30	0.02	3.5	3.7	1.07	220	99	−61
2[g]	**Pd1**	15	1.62	0.08	14.0	16.2	1.16	218	99	−60
3	**Pd1**	30	1.04	0.42	18.9	20.4	1.08	201	98	−62
4	**Pd1**	50	5.10	2.04	42.7	62.8	1.47	175	94	−62
5	**Pd1**	70	5.47	2.19	29.7	46.6	1.57	149	91	−65
6	**Pd1**	90	4.00	1.60	22.3	32.6	1.46	145	90	−64
7	**Pd1**	110	2.19	0.88	8.9	14.7	1.64	130	88	−63
8	**Pd1**	130	1.77	0.71	6.3	12.8	2.03	125	85	−61
9[h]	**Pd1**	50	4.74	1.19	75.3	118.5	1.57	188	–[j]	−62
10[i]	**Pd1**	50	2.77	0.69	90.4	157.3	1.74	189	–[j]	−62
11	**Pd2**	30	0.12	0.05	5.6	7.2	1.28	85	–[j]	–[j]
12	**Pd2**	50	0.98	0.39	8.9	19.4	2.18	88	–[j]	–[j]
13	**Pd2**	70	0.36	0.14	7.2	15.8	2.20	84	–[j]	–[j]
14	**Pd2**	90	trace	–	–	–	–	–	–	–

[a] Reaction conditions: Pd catalyst (5 μmol), NaBArF (1.5 equiv), toluene/CH_2Cl_2 (98 mL/2 mL), ethylene (8 bar), polymerization time (30 min); all entries are based on at least two runs, unless noted otherwise. [b] Activity has the units of g mol^{-1} h^{-1}. [c] Determined by gel permeation chromatography (GPC) in 1,2,4-trichlorobenzene at 150 °C using a light-scattering detector. [d] Number of branches per 1000 C (brs), as determined by ^{1}H NMR spectroscopy. [e] The ratio of Me branches in total branches, determined by ^{13}C NMR spectroscopy. [f] Determined by differential scanning calorimetry (DSC, second heating). [g] Pd catalyst (10 μmol), polymerization time (2 h). [h] Pd catalyst (2 μmol), toluene/CH_2Cl_2 (148 mL/2 mL), polymerization time (2 h). [i] Pd catalyst (0.5 μmol), toluene/CH_2Cl_2 (148 mL/2 mL), polymerization time (8 h). [j] Not determined.

Pd2 produced polyethylenes with virtually identical degrees of branching (ca. 86/1000 C) over the entire temperature range studied (30 °C to 70 °C; Table 1, entries 11–13). One tentative explanation for the decreased degrees of branching with elevated temperature is that the activation entropy ($\Delta S^{\neq}$) of ethylene insertion into a 2-alkyl-Pd species is much more negative than that for insertion into a 1-alkyl-Pd species.[30] Considering the branching pattern, **Pd1** is extremely selective in forming methyl branches exclusively at lower temperatures. Only at elevated temperatures of 50 °C and higher, longer branches including Et, Pr, *n*Bu, *s*Bu, and C_{4+} are formed to a significant extent (Supporting Information, Figure S7).

The formation of polyethylenes with ultrahigh branching occurs in a living fashion at polymerization temperatures of 0 °C to 30 °C, as indicated by narrow molecular weight distributions (polydispersity index (PDI) = 1.07–1.16). This is further corroborated by polymerizations with prolonged reactions times (Table 2). Both yield and the M_n increase linearly with time (Figure 3). Molecular weight distributions remain very narrow, even over two hours of polymerization, to afford very high molecular weights (M_n = 700 kg mol^{-1} at M_w/M_n = 1.12 and ca. 200 branches/1000 C); moreover, degrees of branching are virtually identical (Figure 3c). Notably, the polymer product obtained is elastic and highly transparent because of the combination of very high molecular weight and high branching (Figure 3d).

Studies of the influence of ethylene pressure on polymerization (Table 2, entries 1 and 5–7) showed that, in the range from 2 bar to 8 bar investigated, branching remains unaltered, and both activity and polymer molecular weight increase only slightly. Activity and polymer molecular weight level off at ≥ 4 atm, and a saturation regime is attained. This suggests that the catalyst resting state is an alkyl–olefin complex (see the proceeding text).

Ultrahigh Branching of Main-Chain-Functionalized Polyethylenes. The copolymerization of ethylene with methyl acrylate (MA) has been studied extensively with cationic α-diimine Pd^{II} species.[18,19,23,24,28,29,31–35] In the branched copolymers formed, the ester groups are located preferentially at the ends of branches (Figure 1E). Stoichiometric NMR studies showed that these structures result from 2,1-insertion of MA, followed by chain walking.[18,19]

The catalytic copolymerization properties of **Pd1** toward ethylene and MA were studied at various temperatures and times, employing 1.0 M MA and radical inhibitor galvinoxyl (Table 3). Elevating the reaction temperature from 30 °C to 90 °C resulted in an increase of activity, polymer molecular weight, as well as MA incorporation (Table 3, entries 1–4). At 90 °C polymerization temperature the molecular weight reaches 85 kg mol^{-1} and the MA incorporation reaches 1.5 mol %. Prolonged reaction times lead to an increase of yield and polymer molecular weight

Table 2: Effect of time and pressure on ethylene polymerization with α-diimine **Pd1**.[a]

Entry	p [bar]	t [min]	Yield [g]	Act. [$\times 10^6$][b]	M_n [$\times 10^4$][c]	M_w/M_n[c]	Brs[d]	T_g[e] [°C]
1	8	30	1.04	0.42	18.9	1.08	204	−62
2	8	60	2.01	0.40	35.7	1.06	205	−62
3	8	90	3.21	0.43	52.6	1.08	202	−60
4	8	120	4.18	0.42	69.7	1.12	196	−60
5	6	30	1.00	0.40	17.4	1.12	206	−61
6	4	30	0.90	0.36	17.5	1.13	206	−61
7	2	30	0.72	0.29	15.1	1.08	207	−60

[a] Reaction conditions: Pd catalyst (5 μmol), NaBArF (1.5 equiv), toluene/CH_2Cl_2 (98 mL/2 mL), ethylene (8 bar), temperature (30 °C), polymerization time (30 min); all entries are based on at least two runs, unless noted otherwise. [b] Activity has the units of g mol^{-1} h^{-1}. [c] Determined by GPC in 1,2,4-trichlorobenzene at 150 °C using a light-scattering detector. [d] Number of branches per 1000 C (brs), as determined by ^{1}H NMR spectroscopy. [e] Determined by DSC (second heating).

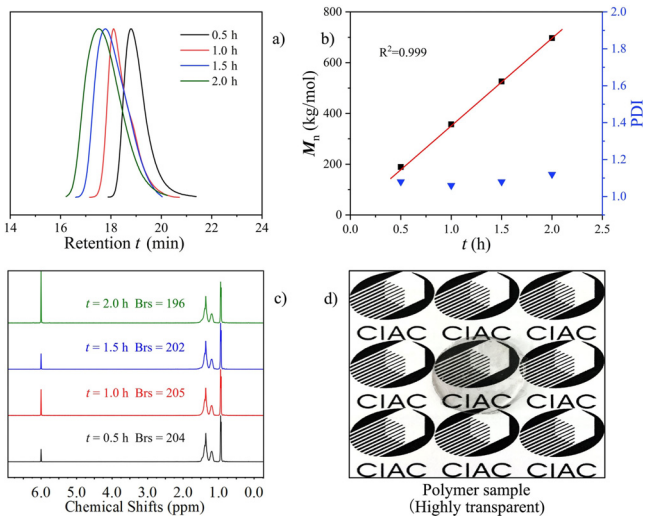

Figure 3. a,b) Living ethylene polymerization with **Pd1** at 30 °C (Table 2, entries 1–4). c) ^{1}H NMR spectra of polyethylenes (Table 2, entries 1–4). d) Appearance of as-obtained highly branched polyethylene sample (Table 2, entry 1).

at an unaltered MA incorporation (Table 3, entries 2 vs. 5, entry 3 vs. 6), indicating both excellent thermal stability and functional group tolerance of the catalyst.

The microstructure of the copolymers was unraveled by comprehensive ^{1}H, ^{13}C, ^{1}H,^{1}H COSY, ^{1}H,^{13}C HSQC, and ^{1}H,^{13}C HMBC NMR spectroscopy (Supporting Information). In view of the strong propensity for branch formation observed in ethylene polymerization, in-chain incorporation of MA (M_{MA})[36,37] is overwhelmingly favored over incorporation at the end of branches (T_{MA}).

Key ^{13}C NMR resonances pertaining to M_{MA} units are 177.23 ppm and 51.42 ppm, corresponding to the carbonyl group (C=O) and methoxy moiety (MeO), respectively. By comparison, the T_{MA} unit exhibits signals at 174.44 ppm and 51.57 ppm. Assignment of the indicative α-CH (CH_M) moiety ($\delta_H \approx 2.33$ ppm, $\delta_C \approx 46.00$ ppm) in M_{MA} units is unambiguously confirmed by ^{1}H,^{13}C HSQC (plus DEPT135) and was determined by ^{1}H,^{13}C HMBC to be adjacent to C=O group of the ester moiety. By comparison, the α-CH_2 carbon atom adjacent to the ester group in the T_{MA} unit resonates at $\delta_C \approx 34.35$ ppm. These conclusive and independent assignments are consistent with previous observations.[36]

At 30 °C polymerization temperature, in-chain incorporation is virtually the exclusive mode of incorporation (M_{MA}:T_{MA} = 98:2) and, even at high temperatures, a high selectivity is retained (at 90 °C, 89:11; Figure 4). A preferred in-chain incorporation by the α-diimine Pd^{II} system was first observed for Takeuchi and Osakada's double-decker dinuclear complex (M_{MA}:T_{MA} = 85:15), forming a moderately branched (47/1000 C) copolymer. By comparison, its mononuclear Pd^{II} analogue afforded the common T_{MA} units (M_{MA}:T_{MA} = 21:79).[36]

Comparing the microstructures formed to other catalyst systems, previously reported α-diimine Pd^{II} catalysts produce highly branched copolymers with functional groups located at the end of branches (Figure 1E).[23] Neutral PO-coordinated Pd^{II} complexes, another seminal catalyst type, afford linear copolymers with functional groups incorporated into the chain (Figure 1D).[38–49] By contrast, our catalyst **Pd1** enables acrylate in-chain incorporation in highly branched copolymers (Figure 1F).

Mechanistic Insights. These highly unusual polymer microstructures formed with **Pd1** call for a mechanistic rationale. To this end, stoichiometric MA insertion reactions with **Pd1** species were monitored by NMR spectroscopy, employing the cationic acetonitrile-coordinated **Pd1-(CH$_3$CN)**$^+$ as a precursor. Notably, the coordinated CH_3CN

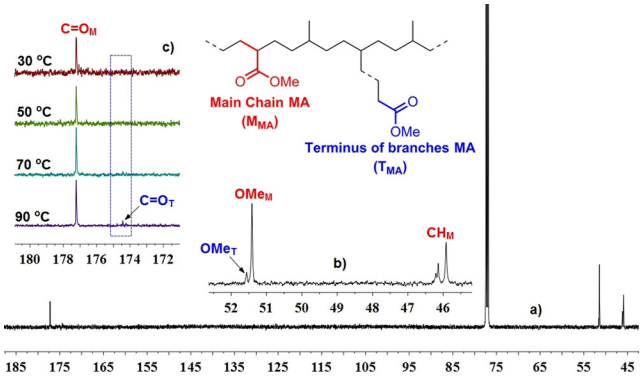

Figure 4. ^{13}C NMR spectra (500 MHz, 298 K, $CDCl_3$) of ethylene—MA copolymers. a) Key signals (45–185 ppm) of ethylene—MA copolymer produced at 90 °C (Table 3, entry 4). b) Magnification of signals (45–53 ppm). c) Comparison of C=O resonances of M_{MA} and T_{MA} at differed reaction temperatures (30, 50, 70, and 90 °C; Table 3, entries 1–4).

Table 3: Copolymerization of ethylene and MA with **Pd1**.[a]

Entry	*t* [h]	*T* [°C]	Yield [g]	Act. [×10^4][b]	M_n [×10^4][c]	M_w [×10^4][c]	M_w/M_n[c]	Brs[d]	X_{MA} [mol%][e]	M_{MA}:T_{MA}[f]
1	8	30	0.15	0.19	1.9	2.5	1.36	213	0.6	98:2
2	8	50	0.34	0.43	3.6	4.7	1.32	193	0.9	96:4
3	8	70	0.66	0.82	5.5	7.3	1.32	173	1.3	94:6
4	8	90	1.18	1.48	8.5	12.6	1.48	158	1.5	89:11
5	2	50	0.10	0.50	1.8	2.3	1.29	199	0.9	95:5
6	2	70	0.28	1.40	2.8	3.4	1.22	177	1.1	93:7

[a] Reaction conditions: Pd catalyst (10 μmol), NaBArF (1.5 equiv), galvinoxyl (5.0 equiv), toluene/CH_2Cl_2 (28 mL/2 mL), ethylene (8 bar), MA (1.0 M); all entries are based on at least two runs, unless noted otherwise. [b] Activity has the units of g mol^{-1} h^{-1}. [c] Determined by GPC in 1,2,4-trichlorobenzene at 150 °C using a light-scattering detector. [d] Number of branches per 1000 C (brs), as determined by ^{1}H NMR spectroscopy. [e] X_{MA} = Incorporation of MA in copolymer, as determined by ^{1}H NMR spectroscopy. [f] The ratio of MA incorporated into the main chain of the copolymer and MA incorporated at the end of branches of copolymer T_{MA} (M_{MA}:T_{MA}), as determined by ^{13}C NMR spectroscopy.

molecule of **Pd1(CH$_3$CN)**$^+$ exhibits resonances at unusually high fields (^{1}H: −0.05 ppm; ^{13}C: −1.50 ppm) in the NMR spectra (Supporting Information), again indicating shielding (this compares to a ^{1}H shift of 1.77 ppm in **Pd2(CH$_3$CN)**$^+$).[18] Monitoring the reaction of **Pd1(CH$_3$CN)**$^+$ with 15 equivalents of MA revealed the formation of two insertion products, albeit in a slow reaction (50 % conversion after 48 h) because of strong relative binding of acetonitrile. Alternatively, mixing **Pd1** and NaBArF with 10 equivalents of MA produces the same two insertion products (in a ca. 9:1 ratio) much more quickly (complete conversion within 10 min).

Comprehensive 1D and 2D NMR spectroscopy, attenuated total reflection infrared spectroscopy (ATR-IR), electrospray ionization mass spectrometry (ESI-MS), and elemental analysis reveals the major product to be the five-membered chelate **Pd1(MA)-Five**, and **Pd1(MA)-Six** the minor product (Figure 5; Supporting Information). As a notable feature, shielding by the iptycene aryls is reflected in the esters' MeO resonances at 1.79 ppm and 1.06 ppm, respectively (Figure 6); this compares to 3.0–3.7 ppm in chelates with common α-diimines). The identity and structure of **Pd1(MA)-Five** was further elaborated by single-crystal X-ray diffraction analysis (Figure 6a).

The finding of **Pd1(MA)-Five**, formed by 1,2-insertion of MA as the major product (82:18) is unexpected, as with Pd^{II} α-diimine complexes 2,1-insertion is the much preferred pathway (Figure 5b). Correspondingly, for MA insertion with **Pd2** we observed **Pd2(MA)-Six** as the expected major product (13:87), in agreement with Brookhart et al.[18,19] and studies of other α-diimine complexes.[24,33,34] Note that Takeuchi and Osakada also assume a preferred 2,1-insertion for their aforementioned double-decker complex, the origin of the partial in-chain incorporation rather being an interaction of the monomer with the second Pd center (Supporting Information, Figure S2).[36]

The insertion of MA into Pd–C bonds generally occurs with 2,1-regioselectivity for electronic reasons.[21] The nucleophilic Pd-alkyl group migrates to the more electron deficient terminal olefinic carbon of the acrylate. A rare case of a preferred 1,2-insertion was observed in stoichiometric reactions of bulky substituted neutral diazaphospholidine–sulfonato Pd^{II} complexes.[50,51] In this particular case, destabilization of the transition state of 2,1-insertion by steric interference with the diazaphospholidine substituents is the origin of the inverted regioselectivity. Unfortunately, these complexes were not active for ethylene–acrylate copolymerization.[50,51]

In summary, branch formation in catalytic ethylene homopolymerization occurs by chain walking; that is, a series of β-H elimination, olefin rotation in the resulting

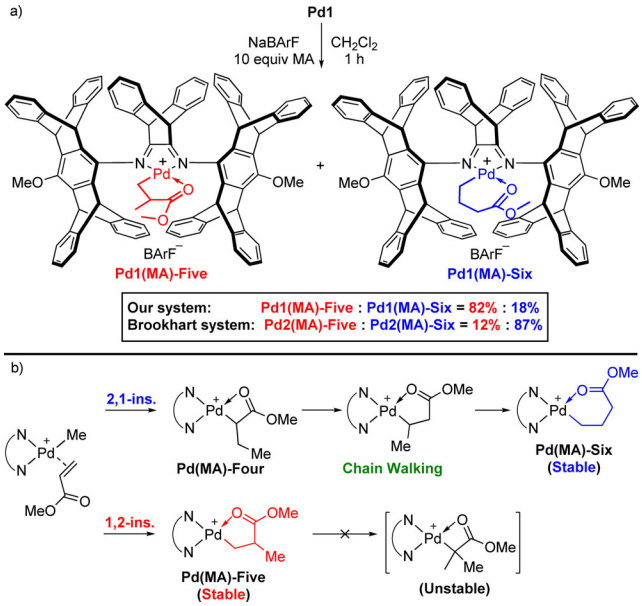

Figure 5. a) Isolated MA insertion products. b) Acrylate insertion pathways.

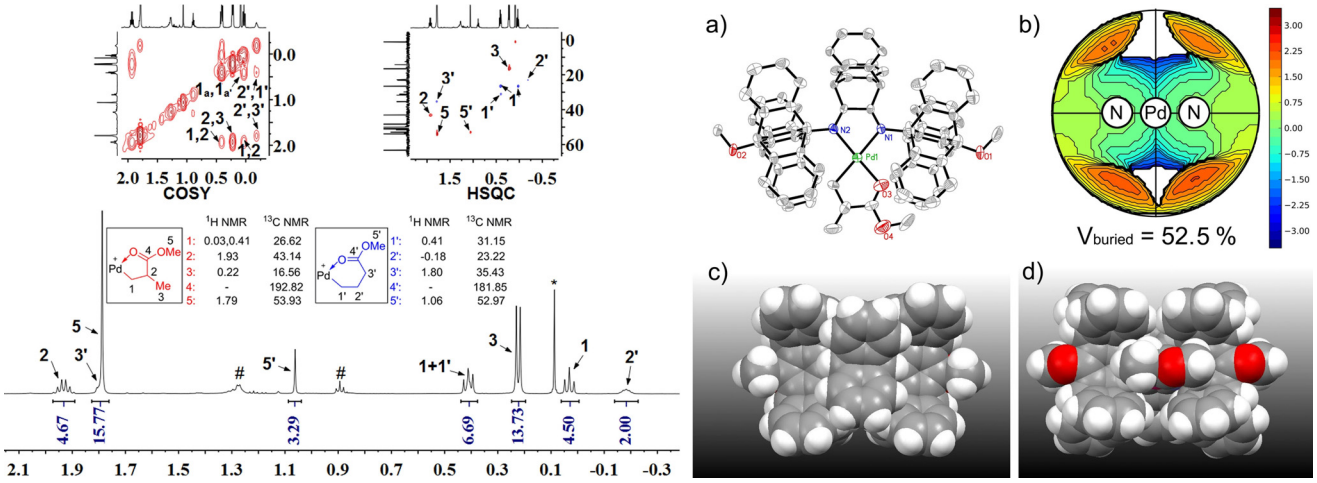

Figure 6. Left: NMR spectra (500 MHz, 298 K, $CDCl_3$) of MA insertion products **Pd1(MA)-Five** and **Pd1(MA)-Six** (hexane (#), silicone grease (*)). Right: a) molecular structure of 1,2-MA insertion product **Pd1(MA)-Five** drawn with 30% probability ellipsoids; the anion part BArF$^-$ has been removed; b) steric map of **Pd1(MA)-Five** (view from bottom to top); c) space-filling model of **Pd1(MA)-Five** (view from top to bottom); d) space-filling model of **Pd1(MA)-Five** (view from bottom to top).

metal–hydride olefin complex, and reinsertion with opposite regiochemistry to the previous β-H elimination. Such pathways are highly accessible for **Pd1**, as evidenced by the unprecedented high degrees of branching. Peculiarly, however, at the same time branch formation is selective and restricted to formation of methyl branches. Furthermore, despite the extreme propensity for chain walking, acrylate incorporation occurs in-chain highly selectively. This can be traced back to a 1,2-regioselective insertion of acrylate, which contrasts other cationic Pd^{II} α-diimine complexes. Thus, the seemingly contradictive polymer microstructure can be accounted for by a conclusive mechanistic picture (Figure 7). In the unique steric environment provided by the rigid **DBB-Ipty** framework, chain walking is rapid and competitive with chain growth.[52] However, this steric constraint and rigid framework selectively limits the viable insertion events in the alkyl olefin species, namely to ethylene insertion into 2-alkyls (in addition to terminal alkyls) and to acrylate insertion in a 1,2-fashion. Ethylene insertion into *n*-alkyls (n > 2) and 2,1-insertion of acrylate are disfavored, likely by steric constraints imposed by the ligand rigid framework destabilizing the more spatially demanding transition states.

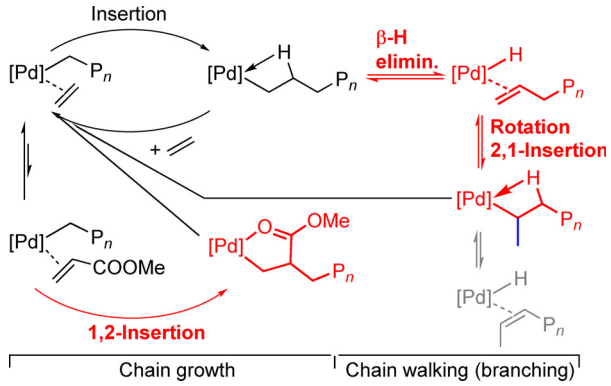

Figure 7. Mechanism of chain growth and branching with specific features promoted (red bold) and suppressed (gray) by the **DBB-Ipty** environment.

Regarding the polymers formed by **Pd1** from a synthesis point of view, their ultrahigh branching resembles the microstructure of commercial EP rubbers and allows access to such materials with ethylene as the sole monomer and also with polar functional groups. These are desirable prospective features.

Acknowledgements

The authors are thankful for financial support from the National Natural Science Foundation of China (No. 21871250), the Jilin Provincial Science and Technology Department Program (Nos. 20190201009JC, 20200801009GH), and Shaanxi Provincial Natural Science Basic Research Program-Shaanxi Coal and Chemical Industry Group Co., Ltd. Joint Fund (No. 2019JLZ-02). We thank Qingbin He and Prof. Quan Chen from CIAC for additional polymer analysis. Open access funding enabled and organized by Projekt DEAL.

Conflict of interest

The authors declare no conflict of interest.

Keywords: coordination polymerization · homogeneous catalysis · palladium catalysts · polyolefins · ultrahigh branching

[1] J. M. Eagan, J. Xu, R. Di Girolamo, C. M. Thurber, C. W. Macosko, A. M. LaPointe, F. S. Bates, G. W. Coates, *Science* **2017**, *355*, 814–816.
[2] P. D. Hustad, *Science* **2009**, *325*, 704–707.
[3] M. Stürzel, S. Mihan, R. Mülhaupt, *Chem. Rev.* **2016**, *116*, 1398–1433.
[4] M. C. Baier, M. A. Zuideveld, S. Mecking, *Angew. Chem. Int. Ed.* **2014**, *53*, 9722–9744; *Angew. Chem.* **2014**, *126*, 9878–9902.
[5] T. Liang, S. B. Goudari, C. Chen, *Nat. Commun.* **2020**, *11*, 372.
[6] M. Schnitte, A. Staiger, L. A. Casper, S. Mecking, *Nat. Commun.* **2019**, *10*, 2592.
[7] A. L. Kocen, M. Brookhart, O. Daugulis, *Nat. Commun.* **2019**, *10*, 438.
[8] C. Boucher-Jacobs, M. Rabnawaz, J. S. Katz, R. Even, D. Guironnet, *Nat. Commun.* **2018**, *9*, 841.
[9] Y. Gao, J. Chen, Y. Wang, D. B. Pickens, A. Motta, Q. J. Wang, Y. Chung, T. L. Lohr, T. J. Marks, *Nat. Catal.* **2019**, *2*, 236–242.
[10] T. R. Younkin, E. F. Connor, J. I. Henderson, R. H. Grubbs, D. A. Bansleben, *Science* **2000**, *287*, 460–462.
[11] C. Chen, *Nat. Rev. Chem.* **2018**, *2*, 6–14.
[12] A. Keyes, H. E. Basbug Alhan, E. Ordonez, U. Ha, D. B. Beezer, H. Dau, Y. S. Liu, E. Tsogtgerel, G. R. Jones, E. Harth, *Angew. Chem. Int. Ed.* **2019**, *58*, 12370–12391; *Angew. Chem.* **2019**, *131*, 12498–12520.
[13] C. Wang, Z. Hou, *Sci. Adv.* **2017**, *3*, e1701011.
[14] H. Mu, L. Pan, D. Song, Y. Li, *Chem. Rev.* **2015**, *115*, 12091–12137.
[15] N. K. Boaen, M. A. Hillmyer, *Chem. Soc. Rev.* **2005**, *34*, 267–275.
[16] B. K. Long, J. M. Eagan, M. Mulzer, G. W. Coates, *Angew. Chem. Int. Ed.* **2016**, *55*, 7106–7110; *Angew. Chem.* **2016**, *128*, 7222–7226.
[17] L. K. Johnson, C. M. Killian, M. Brookhart, *J. Am. Chem. Soc.* **1995**, *117*, 6414–6415.
[18] L. K. Johnson, S. Mecking, M. Brookhart, *J. Am. Chem. Soc.* **1996**, *118*, 267–268.
[19] S. Mecking, L. K. Johnson, L. Wang, M. Brookhart, *J. Am. Chem. Soc.* **1998**, *120*, 888–899.
[20] Z. Guan, P. M. Cotts, E. F. McCord, S. J. McLain, *Science* **1999**, *283*, 2059–2062.
[21] A. Nakamura, S. Ito, K. Nozaki, *Chem. Rev.* **2009**, *109*, 5215–5244.
[22] A. Nakamura, T. M. Anselment, J. Claverie, B. Goodall, R. F. Jordan, S. Mecking, B. Rieger, A. Sen, P. W. van Leeuwen, K. Nozaki, *Acc. Chem. Res.* **2013**, *46*, 1438–1449.
[23] Z. Chen, M. Brookhart, *Acc. Chem. Res.* **2018**, *51*, 1831–1839.
[24] S. Zhong, Y. Tan, L. Zhong, J. Gao, H. Liao, L. Jiang, H. Gao, Q. Wu, *Macromolecules* **2017**, *50*, 5661–5669. In this paper, a Pd catalyst generates PEs with high degrees of branching (ca. 100/1000 C), which remain almost unchanged at various temper-

atures. It also indicates that a higher steric constraint leads to lower degrees of branching compared to our Pd system.
[25] Y. Liao, Y. Zhang, L. Cui, H. Mu, Z. Jian, *Organometallics* **2019**, *38*, 2075 – 2083.
[26] L. Falivene, Z. Cao, A. Petta, L. Serra, A. Poater, R. Oliva, V. Scarano, L. Cavallo, *Nat. Chem.* **2019**, *11*, 872 – 879.
[27] D. J. Tempel, L. K. Johnson, R. L. Huff, P. S. White, M. Brookhart, *J. Am. Chem. Soc.* **2000**, *122*, 6686 – 6700.
[28] S. Dai, X. Sui, C. Chen, *Angew. Chem. Int. Ed.* **2015**, *54*, 9948 – 9953; *Angew. Chem.* **2015**, *127*, 10086 – 10091.
[29] S. Dai, C. Chen, *Angew. Chem. Int. Ed.* **2016**, *55*, 13281 – 13285; *Angew. Chem.* **2016**, *128*, 13475 – 13479.
[30] D. Bézier, O. Daugulis, M. Brookhart, *Organometallics* **2017**, *36*, 443 – 447.
[31] L. Zhong, H. Zheng, C. Du, W. Du, G. Liao, C. S. Cheung, H. Gao, *J. Catal.* **2020**, *384*, 208 – 217.
[32] K. E. Allen, J. Campos, O. Daugulis, M. Brookhart, *ACS Catal.* **2015**, *5*, 456 – 464.
[33] C. S. Popeney, D. H. Camacho, Z. Guan, *J. Am. Chem. Soc.* **2007**, *129*, 10062 – 10063.
[34] C. S. Popeney, Z. Guan, *J. Am. Chem. Soc.* **2009**, *131*, 12384 – 12393.
[35] F. Zhai, J. B. Solomon, R. F. Jordan, *Organometallics* **2017**, *36*, 1873 – 1879.
[36] S. Takano, D. Takeuchi, K. Osakada, N. Akamatsu, A. Shishido, *Angew. Chem. Int. Ed.* **2014**, *53*, 9246 – 9250; *Angew. Chem.* **2014**, *126*, 9400 – 9404.
[37] A. Dall'Anese, V. Rosar, L. Cusin, T. Montini, G. Balducci, I. D'Auria, C. Pellecchia, P. Fornasiero, F. Felluga, B. Milani, *Organometallics* **2019**, *38*, 3498 – 3511.
[38] S. Luo, J. Vela, G. R. Lief, R. F. Jordan, *J. Am. Chem. Soc.* **2007**, *129*, 8946 – 8947.
[39] T. Kochi, S. Noda, K. Yoshimura, K. Nozaki, *J. Am. Chem. Soc.* **2007**, *129*, 8948 – 8949.
[40] W. Weng, Z. Shen, R. F. Jordan, *J. Am. Chem. Soc.* **2007**, *129*, 15450 – 15451.
[41] D. Guironnet, P. Roesle, T. Runzi, I. Gottker-Schnetmann, S. Mecking, *J. Am. Chem. Soc.* **2009**, *131*, 422 – 423.
[42] S. Ito, K. Munakata, A. Nakamura, K. Nozaki, *J. Am. Chem. Soc.* **2009**, *131*, 14606 – 14607.
[43] T. Rünzi, D. Fröhlich, S. Mecking, *J. Am. Chem. Soc.* **2010**, *132*, 17690 – 17691.
[44] B. P. Carrow, K. Nozaki, *J. Am. Chem. Soc.* **2012**, *134*, 8802 – 8805.
[45] Y. Ota, S. Ito, J. Kuroda, Y. Okumura, K. Nozaki, *J. Am. Chem. Soc.* **2014**, *136*, 11898 – 11901.
[46] B. S. Xin, N. Sato, A. Tanna, Y. Oishi, Y. Konishi, F. Shimizu, *J. Am. Chem. Soc.* **2017**, *139*, 3611 – 3614.
[47] Y. Zhang, H. Mu, L. Pan, X. Wang, Y. Li, *ACS Catal.* **2018**, *8*, 5963 – 5976.
[48] W. Zhang, P. M. Waddell, M. A. Tiedemann, C. E. Padilla, J. Mei, L. Chen, B. P. Carrow, *J. Am. Chem. Soc.* **2018**, *140*, 8841 – 8850.
[49] C. Tan, C. Chen, *Angew. Chem. Int. Ed.* **2019**, *58*, 7192 – 7200; *Angew. Chem.* **2019**, *131*, 7268 – 7276.
[50] P. Wucher, L. Caporaso, P. Roesle, F. Ragone, L. Cavallo, S. Mecking, I. Gottker-Schnetmann, *Proc. Natl. Acad. Sci. USA* **2011**, *108*, 8955 – 8959.
[51] P. Wucher, P. Roesle, L. Falivene, L. Cavallo, L. Caporaso, I. Göttker-Schnetmann, S. Mecking, *Organometallics* **2012**, *31*, 8505 – 8515.
[52] Another potential possibility is that chain walking is neither fast nor excessive, while ethylene insertion into the 2-alkyl-Pd group is fast and comparable with that into the 1-alkyl-Pd group.

Manuscript received: April 2, 2020
Revised manuscript received: May 9, 2020
Accepted manuscript online: May 22, 2020
Version of record online: July 6, 2020

